Available online at www.sciencedirect.com
ScienceDirect
Polymer 48 (2007) 7049–7057
polymer
www.elsevier.com/locate/polymer

Poly[(2-ethylhexyl acrylate)-*ran*-(*tert*-butyl acrylate)]-*block*-poly(2-cinnamoyloxyethyl acrylate) synthesis and properties

Ronghua Zheng [a], Guojun Liu [a,*], Tze-Chi Jao [b]

[a] *Department of Chemistry, Queen's University, 90 Bader Lane, Kingston, Ontario K7L 3N6, Canada*
[b] *Fundamental Research Group, Afton Chemical Corporation, 500 Spring Street, Richmond, VA 23219, USA*

Received 27 September 2007; accepted 5 October 2007
Available online 12 October 2007

Abstract

Poly[(2-ethylhexyl acrylate)-*ran*-(*tert*-butyl acrylate)]-*block*-poly(2-cinnamoyloxyethyl acrylate) or P(EXA-*r*-*t*BA)-PCEA was synthesized by atom transfer radical polymerization. Reactivity ratios of EXA and *t*BA for copolymerization were determined. The specific refractive index increments of six diblocks were measured as a function of their composition. The diblocks were thermally stable and formed micelles in an automobile engine oil. Such micelles may be useful as an anti-friction additive in lubricating oils.

Keywords: Atom transfer radical polymerization; Block copolymers; Micellization

1. Introduction

Over the past decade the field of atom transfer radical polymerization [1] (ATRP) has witnessed explosive growth and it has now been used to polymerize a wide range of monomers [2] and to make block copolymers [2]. The easier accessibility of block copolymers by ATRP [3,4,5] has in turn helped fuel the study of block copolymer self-assembly in block-selective solvents. Block copolymers self-assemble into nanoaggregates with tens of morphologies ranging from spheres [6,7] to cylinders [8–10], tubes [11–15], vesicles [9,10,16–19], donuts [10,20,21], and many others [22]. Despite many prior studies, we failed to find in the literature formulations for block copolymer nanoaggregates that not only disperse in lubricant oils but also bind effectively to stainless steel surfaces because these two requirements are conflicting. While dispersion in lubricant oils requires nonpolar polymers [23] for the low polarity of the oils, which typically consist of paraffins, aromatics, and naphthalenes [24], steel binding typically requires relatively polar segments. Reported in this paper is the preparation and characterization of poly[(2-ethylhexyl acrylate)-*ran*-(*tert*-butyl acrylate)]-*block*-poly(2-cinnamoyloxyethyl acrylate) or P(EXA-*r*-*t*BA)-PCEA that should meet this requirement and may be used in lubricant oils as a friction reduction agent, where PEXA and PCEA are oil soluble and insoluble, respectively, and the *t*BA units can be hydrolyzed to yield acrylic acid groups that are metal-binding [25]. Also reported in this paper are some thermal and optical properties of the diblocks synthesized.

2. Experimental section

2.1. Materials and reagents

N,*N*,*N*′,*N*″,*N*″-Pentamethyldiethylenetriamine (PMDETA) (99%), 2-ethylhexyl acrylate (EXA, 98%), *tert*-butyl acrylate (*t*BA, 98%), methyl 2-bromopropionate (MBP, 98%), diisopropylamine (99.5%), 1-bromohexane, toluene-d_8 (tol-d_8, 99.6% d), and pyridine (99+%) were purchased from Aldrich. EXA was washed by 5% NaOH aqueous solution thrice to remove stabilizer and then dried over anhydrous $MgSO_4$ overnight. It was distilled under vacuum over CaH_2 prior to use. Monomer *t*BA was distilled over CaH_2. PMDETA, tol-d_8, and diisopropylamine were distilled prior to use. MBP and

* Corresponding author.
E-mail address: gliu@chem.queensu.ca (G. Liu).

0032-3861/$ - see front matter © 2007 Elsevier Ltd. All rights reserved.
doi:10.1016/j.polymer.2007.10.010

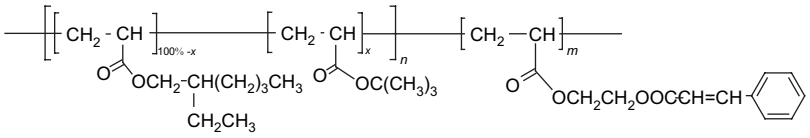

1-bromohexane were distilled under vacuum. Pyridine was dried by refluxing with CaH_2 and distilled prior to use. Monomer 2-trimethylsiloxyethyl acrylate (HEA-TMS) [26] and ligand 4,4′-diheptyl-2,2′-bipyridine (dHbip) [27] were synthesized following literature methods. All reagents used in polymerization were stored under Ar after purification. Cinnamoyl chloride (98%), 4,4′-dimethyl-2,2′-bipyridine, *n*-butyllithium (2.5 M in hexanes), CuBr (99.999%), $CuBr_2$ (99.999%) were purchased from Aldrich and used as received. The lubricant base oil used was EHC-45, a product of Imperial Oil and supplied by Afton Chemical Corporation. It is a hydrocracked group II base oil characterized by high saturated hydrocarbon content (95%), high viscosity and low volatility. Our experiments yielded a refractive index of 1.4667 at the sodium D line and a viscosity of 36.3 cP at 22 °C for the oil [28].

2.2. Preparation and fractionation of P(EXA-r-tBA)

In an example preparation we started by adding 110.6 mg (0.77 mmol) of CuBr and 9.2 mg (0.041 mmol) of $CuBr_2$ into an argon-purged 250-mL round-bottom flask. The flask was evacuated and refilled by Ar and this procedure was repeated twice before 5.0 mL of toluene, 30.0 mL (26.5 g, 144 mmol) of EXA, and 0.32 mL (0.28 g, 2.2 mmol) of *t*BA were added. Also added were 858.9 mg (2.44 mmol) of dHbip dissolved in 10.0 mL of toluene and 90.6 μL (135.6 mg, 0.81 mmol) of methyl 2-bromopropionate (MBP). The mixture was cooled down to −78 °C, evacuated, thawed, and refilled with Ar. The procedure was repeated twice before the flask was immersed in an oil bath preheated at 85 °C. The polymerization was performed at this temperature for 4.5 days. After cooling to room temperature, the mixture was diluted with 300 mL of THF and filtered through a column of neutral alumina to remove the catalyst. The filtrate was concentrated by rota-evaporation to 200 mL and polymer yield was 89%.

To fractionate the polymer, 160 mL of methanol was added dropwise to the filtrate so that the solution just turned cloudy. The resultant solution was left standing overnight at room temperature to yield two phases. The denser bottom layer was collected. To the top layer was added another 5.0 mL of methanol before it was left standing overnight at 2 °C. The bottom dense layer was collected and added into methanol to precipitate out the polymer. The collected precipitate was dried in vacuum oven at 40 °C for 10 h to yield 17.6 g of polymer at 66% yield.

2.3. Reactivity ratios of EXA and tBA

Copolymerization reactivity ratios r_{EXA} and r_{tBA} were determined in tol-d_8 at the *t*BA to EXA molar feed ratios of 1/19 and 19/1, respectively. To determine r_{EXA} added into an argon-purged 100-mL round-bottom flask were 22.1 mg (0.154 mmol) of CuBr, 1.8 mg (0.008 mmol) of $CuBr_2$, 2.0 mL of tol-d_8, 4.81 mL (4.25 g, 23.1 mmol) of EXA, 0.178 mL (156 mg, 1.22 mmol) of *t*BA, 172 mg (0.487 mmol) of dHbip, and 18.1 μL (27.1 mg, 0.162 mmol) of MBP. The mixture was degassed by three freeze–pump–thaw–Ar filling cycles before it was immersed in an oil bath preheated at 91 °C. Samples were taken at pre-designated times and diluted by $CDCl_3$ for ^{1}H NMR analysis to determine EXA and *t*BA conversion.

2.4. Preparation of P(EXA-r-tBA)-PHEA

An example preparation involved first adding into an Ar-filled 100-mL round-bottom flask 6.71 g (0.16 mmol) of P(EXA-*r*-*t*BA)-Br with 220 units of EXA and *t*BA or $n = 220$, 2.0 mL of 2-butanone, 22.2 mg (0.155 mmol) of CuBr, 1.8 mg (0.008 mmol) of $CuBr_2$, 9.68 mL (9.21 g, 48.9 mmol) of HEA-TMS, and 34.0 μL (28.2 mg, 0.163 mmol) of PMDETA. The mixture was freed of oxygen by three freeze–pump–thaw–Ar filling cycles as described above for P(EXA-r-*t*BA)-Br synthesis before the flask was immersed in an oil bath preheated at 60 °C. The polymerization was performed at this temperature for 26 h. After cooling to room temperature, the mixture was diluted with THF and filtered through a column of neutral alumina to remove the catalyst. The filtrate was concentrated by rota-evaporation and the polymer was precipitated by adding into a mixture of water and methanol at v/v = 1/3. The obtained polymer was dried at room temperature for 16 h to yield 11.1 g of a highly viscous gum at a yield of 70% relative to the total amount of macro-initiator and HEA-TMS used. Size exclusion chromatography (SEC) analysis yielded a polydispersity index M_w/M_n of 1.26 and ^{1}H NMR analysis gave a first to second block length ratio *n*/*m* of 0.79. Based on the *n*/*m* ratio, the conversion of the HEA-TMS block was 59%.

To hydrolyze the TMS groups, 9.90 g of the P(EXA-*r*-*t*BA)-P(HEA-TMS) sample was added into a round-bottom flask with a magnetic stirring bar and dissolved in 205 mL of THF. To the mixture were then added 12.8 mL of distilled water and 12.8 mL of acetic acid. The mixture was stirred at room temperature for 12 h before purification by dialysis against THF changed five times over 24 h in a tube with a molecular weight cut-off of 12,000—14,000 (Spectrum Laboratories). THF was removed from the final mixture by rota-evaporation.

2.5. Synthesis of P(EXA-r-tBA)-PCEA

Added into a 100-mL round-bottom flask was 2.5 g (7.2 mmol of HEA units) of the above P(EXA-*r*-*t*BA)-PHEA sample. Also added were 55 mL of dry pyridine and 1.79 g

(10.8 mmol) of cinnamoyl chloride. The mixture was stirred at room temperature for 12 h. It was then centrifuged and filtered to remove the pyridium chloride salt. The supernatant was added into methanol to precipitate the polymer. The polymer was further purified by dissolving it in THF and re-precipitation in methanol. The final precipitate was dried in a vacuum oven at room temperature for 12 h to yield 2.87 g of product at 78% yield.

2.6. Specific refractive index increment dn_r/dc

The refractive indices of solvent THF and polymer solutions in THF with concentration up to 5 mg/mL were measured using an Optilab rEX instrument (Wyatt Technology Corporation) at λ=632 nm. The instrument software generated a graph of the differential refractive indice Δn_r of the samples vs. the concentration of the samples. The specific refractive index increment dn_r/dc of each sample was obtained from the slope of such a graph.

2.7. Thermogravimetric and differential scanning calorimetry analyses

Thermogravimetric analyses (TGA) were performed on a Q500 instrument (TA instruments, Inc.). Samples were loaded onto platinum sample pan and heated from 25 to 600 °C at a heating rate of 10 °C/min under nitrogen. Differential Scanning Calorimetry (DSC) was performed on a DSC Q100 (TA instruments, Inc.). The samples were heated from −60 to 100 °C, then cooled down to −60 °C, and finally heated again to 100 °C for data recording at a heating rate of 10 °C/min under nitrogen.

2.8. Micelle formation

Micelles could be prepared by dispersing P(EXA-*r*-*t*BA)-PCEA in hot cyclohexane (CH) or EHC-45 oil directly. To prepare micelles in EHC-45 oil, the polymer/oil mixture was heated at 80 °C under stirring for 13 h. The micelles in CH were obtained from heating a diblock in CH at 60 °C for 13 h.

2.9. Techniques

NMR was performed with Bruker Avance-300 or Bruker Avance-500 using $CDCl_3$ as solvent. SEC was performed using THF as eluant and a differential refractive index detector. The Waters μ-Styragel® HT-4 and 500 Å columns used were calibrated by polystyrene standards. UV absorbance was measured on a Perkin–Elmer Lamda 2 instrument. Light Scattering (LS) data were obtained with a Brookhaven model 9025 instrument using a He–Ne laser operated at 632.8 nm. Transmission Electron Microscopy (TEM) was performed on Hitachi-7000.

To prepare TEM specimen of micelles prepared in EHC-45, a drop of such a solution was dispensed on water surface. The film was picked up by a nitrocellulose-coated copper grid. The grid was rinsed quickly several times with hexane. Micelles in CH were directly aspirated on nitrocellulose-coated copper grids. The samples were stained by OsO_4 vapor for 1 h before TEM observation.

3. Results and discussion

We prepared the targeted diblocks P(EXA-*r*-*t*BA)-PCEA via several steps. First, the P(EXA-*r*-*t*BA) block with a terminal Br group or P(EXA-*r*-*t*BA)-Br was prepared by controlled atom transfer radical copolymerization (ATRCP). P(EXA-*r*-*t*BA)-Br was then used as the macro-initiator to polymerize HEA-TMS to yield P(EXA-*r*-*t*BA)-P(HEA-TMS). The TMS groups were removed by stirring P(EXA-*r*-*t*BA)-P(HEA-TMS) in THF containing a small amount of water and acetic acid to yield P(EXA-*r*-*t*BA)-PHEA. Finally, P(EXA-*r*-*t*BA)-PHEA was reacted with cinnamoyl chloride to produce the desired diblocks P(EXA-*r*-*t*BA)-PCEA. Aside from discussing diblock synthesis, we will report in this section the determination of reactivity ratios r_{EXA} and r_{tBA} of monomers EXA and *t*BA. We will also describe the dependence of specific refractive index increment dn_r/dc of the diblocks in THF on diblock composition and other properties of the diblocks. We end this section by showing micelle formation from a P(EXA-*r*-*t*BA)-PCEA sample in low polarity solvents CH and EHC-45 oil.

3.1. ATRCP of P(EXA-r-tBA)-Br

Controlled ATRP of *t*BA has been reported by other groups [29–31] and our group [32,33]. Controlled ATRP of EXA has also been reported [34–36]. Thus, EXA and *t*BA should undergo atom transfer radical copolymerization or ATRCP.

When we started this project 3 years ago, Ref. [36] reporting clear evidence for controlled ATRP of EXA was not available yet and we had to experiment with different ligands and polymerization temperatures to produce polymers with low SEC polydispersity M_w/M_n. Table 1 gives recipes for preparation and properties of three P(EXA-*r*-*t*BA) samples that were obtained using MPB as the initiator under optimized conditions. The good correspondence between theoretical number-average molar mass M_n and SEC M_n and the low SEC M_w/M_n suggest that the ATRCP was indeed controlled.

The considerable drop in M_w/M_n of sample 3 relative to sample 2 was reasonable, because ATRCP and ATRP are only controlled and not living polymerizations. At high monomer conversions there are some chain coupling reactions [2]. While EXA and *t*BA ATRCP was controlled, we failed to find reactivity ratios r_{EXA} and r_{tBA} for the two monomers EXA and *t*BA for either classical free radical polymerization or ATRCP. Since the final objective of this research was to prepare diblock nanoparticles containing metal-binding AA groups in the P(EXA-AA) corona and the distribution of AA groups in the corona chains would strongly affect their binding properties, we decided to determine the r_{EXA} and r_{tBA}.

We determined the r_{EXA} and r_{tBA} values following a literature method [37] developed specifically for ATRCP. The starting equation for this method is the following which is

Table 1
Recipes for and properties of several P(EXA-*r*-*t*BA)-Br samples prepared

Sample	V_{EXA} (mL)	Solvent	$V_{solvent}$ (mL)	$[EXA]_0/[tBA]_0$	$[EXA]_0/[MPB]_0$	T (°C)	t (h)	Conversion (%)	Theoretical $M_n \times 10^{-4}$ (g/mol)	SEC $M_n \times 10^{-4}$ (g/mol)	SEC M_w/M_n
1[a]	40.0	Butanone	60.8	98.5/1.5	148	60	48	92	2.5	1.83	1.26
2[b]	30.0	Toluene	45.4	98.5/1.5	177	85	108	89	2.9	2.3	1.25
3[b]	58.3	Toluene	67.6	99.9/0.1	300	85	108	67	3.7	2.9	1.10

[a] Ligand was PMDETA; [initiator]/[ligand]/[Cu]=1/1/1; $[CuBr]/[CuBr_2] = 93/7$.
[b] Ligand used was dHbip; [initiator]/[ligand]/[Cu]=1/3/1; $[CuBr]/[CuBr_2] = 95/5$.

applicable to both ATRCP and classical free radical copolymerization:

$$\frac{d[M_1]}{d[M_2]} = \frac{[M_1]}{[M_2]} \times \frac{r_1[M_1] + [M_2]}{[M_1] + r_2[M_2]} \quad (1)$$

To simplify the equation, the initial monomer 1 concentration $[M_1]_0$ was made experimentally much larger than monomer 2 concentration $[M_2]_0$ so that $r_1[M_1] \gg [M_2]$ and $[M_1] \gg r_2[M_2]$ in Eq. (1) for all data analysed. Under such conditions, the $[M_2]$ and $r_2[M_2]$ terms in the numerator and denominator of Eq. (1) were neglected and the resultant equation could be integrated to yield:

$$\frac{[M_1]}{[M_1]_0} = \left(\frac{[M_2]}{[M_2]_0}\right)^{r_1} \quad (2)$$

where monomer 1 could be either *t*BA or EXA depending on the initial relative concentrations of the two.

In our experiments we used an initial monomer concentration ratio of $[M_1]_0/[M_2]_0 = 19/1$. To facilitate polymerization mixture composition monitoring we used tol-d_8 as the polymerization solvent. This allowed samples taken at different times to be diluted by $CDCl_3$ and then used directly for ^1H NMR analysis. Fig. 1 shows the kinetic data for the copolymerization in tol-d_8 in the presence of excess *t*BA and EXA.

Plots of $\ln([M]_0/[M])$ vs. t are linear initially for ATRCP in the presence of excess *t*BA or EXA in agreement with trends shown by most polymerization systems [2]. At longer times, the data deviated negatively from the straight lines when *t*BA was the monomer in excess. The data deviated positively from the straight lines when EXA was used in excess.

ATRP involving CuBr as the catalyst is typically denoted by the following scheme:

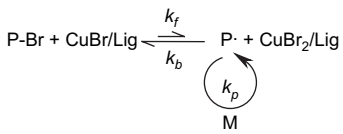

where P, M, and Lig denote polymer, monomer, and ligand, respectively; k_f and k_b denote the rate constants for the forward and backward Br atom transfer reaction; k_p is the chain propagation rate constant. Making the pre-equilibrium assumption on the Br transfer reaction one can show that the rate of a homopolymerization is:

$$-\frac{d[M]}{dt} = k_a[M] \quad (3)$$

where

$$k_a = k_p\left(\frac{k_f}{k_b}\right)[P{-}Br]\frac{[CuBr/Lig]}{[CuBr_2/Lig]} \quad (4)$$

In Eq. (4), [P−Br] is approximately equal to the initiator concentration if the degree of chain termination is low and [CuBr/Lig] and $[CuBr_2/Lig]$ are concentrations of solvated and ligated CuBr and $CuBr_2$, respectively.

Eqs. (3) and (4) were derived for homopolymerization. They should apply at least approximately to the monomer that existed in much excess in our case. Data of Fig. 2 shows that a linear $\ln([M]_0/[M])$-vs.-t plot was observed for both monomers in the early stage of polymerization and thus suggests that k_a was approximately constant then. When data of one monomer started to deviate from the linear $\ln([M]_0/[M])$-vs.-t plot, data of the other monomer followed in synchronization. The data deviated from the $\ln([M]_0/[M])$-vs.-t plot negatively at long times when *t*BA was the major monomer probably mainly for chain termination effect or [P−Br] decrease. This trend is typical of many systems studied in the past [2]. When EXA was the major monomer the kinetic data deviated from the initial linear trend positively. This suggests that k_a increased with monomer conversion. While rate constants k_p, k_f, and k_b might change with monomer conversion, we suspect that increases in $[CuBr/Lig]/[CuBr_2/Lig]$ might be the main culprit for the observed trend because the solubility of $[CuBr_2/Lig]$ should decrease more rapidly than [CuBr/Lig] in a medium which got increasingly rich in P(EXA-*r*-*t*BA)-Br. Such positive data deviation trend is rare but has been observed before for styrene bulk polymerization, for example Ref. [38].

Data of Fig. 1 are re-plotted in Fig. 2 in the form of $[M_1]/[M_1]_0$ vs. $[M_2]/[M_2]_0$. Fitting the data by Eq. (2) yielded $r_{tBA} = 1.17$ and $r_{EXA} = 0.52$. Thus, *t*BA is slightly more reactive than EXA under the polymerization conditions.

An apparent contradiction for data of Figs. 1 and 2 is that polymerization of the mixture containing 95 mol% of *t*BA was slower than that containing 95 mol% EXA while *t*BA is slightly more reactive than EXA as judged from the reactivity ratio values. This can be explained by realizing that different rates were compared in the two cases. The rate of ATRP was governed by the apparent propagation rate constant k_a given in Eq. (4) and the reactivity ratios compare only the

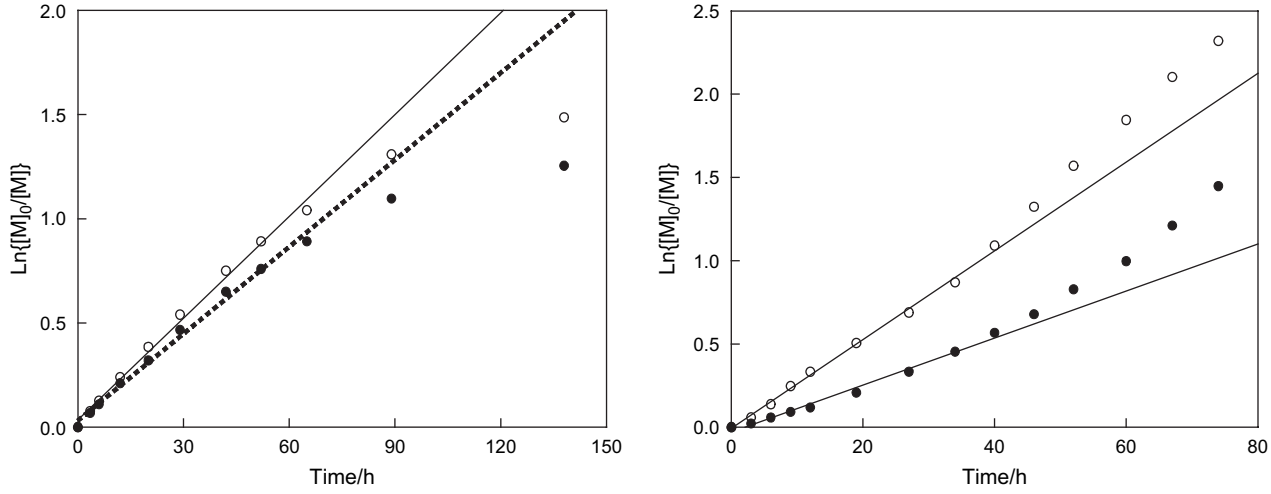

Fig. 1. Plots of ln([M]$_0$/[M]) vs. t for ATRCP of EXA (●) and tBA (○) in the presence of excess tBA (left) and EXA (right), respectively.

magnitudes of the rate constants for chain propagation in a given copolymerization system.

3.2. Fractionation of P(EXA-r-tBA)

While ATRCP yielded P(EXA-*r*-*t*BA)-Br with low M_w/M_n values, we demonstrated that even better defined P(EXA-*r*-*t*BA)-Br samples could be obtained via fractionation precipitation. Such fractionation precipitation was done by adding methanol into a THF solution of P(EXA-*r*-*t*BA)-Br. Table 2 compares the characteristics of a P(EXA-*r*-*t*BA)-Br sample with those of its fractions obtained using the procedure detailed in the Section 2. Fraction 2 of the fractionated sample had not only a lower M_w/M_n value but also was recovered in a high yield of 74%.

3.3. P(EXA-r-tBA)-PCEA

Synthesis of P(EXA-*r*-*t*BA)-PCEA from P(EXA-*r*-*t*BA)-Br required several steps. The first step involved ATRP of HEA-TMS using P(EXA-*r*-*t*BA)-Br to yield P(EXA-*r*-*t*BA)-P(HEA-TMS). P(HEA-TMS) was then hydrolyzed to yield PHEA. P(EXA-*r*-*t*BA)-PCEA was obtained from reacting P(EXA-*r*-*t*BA)-PHEA with cinnamoyl chloride. While controlled ATRP of both HEA-TMS [26,39,40] and HEA [41,42] has been reported before, we took a detour involving P(EXA-*r*-*t*BA)-P(HEA-TMS) synthesis and then P(HEA-TMS) block hydrolysis because it was difficult to find a polymerization solvent that solubilized both P(EXA-*r*-*t*BA) and PHEA.

We found out that HEA-TMS polymerized in butanone at 60 °C yielding P(EXA-*r*-*t*BA)-P(HEA-TMS) with low polydispersity. Fig. 3 compares the SEC trace of a P(EXA-*r*-*t*BA)-Br sample with that of a P(EXA-*r*-*t*BA)-P(HEA-TMS) diblock that was obtained using this P(EXA-*r*-*t*BA)-Br sample as the macro-initiator and was used to yield eventually P(EXA-*r*-*t*BA)-PCEA (sample 4 in Table 3). The clean SEC trace shift shows unambiguously that most of the macro-initiator was active in starting the block copolymerization.

After P(HEA-TMS) hydrolysis and PHEA cinnamation following established procedures [39,43] we obtained a total of

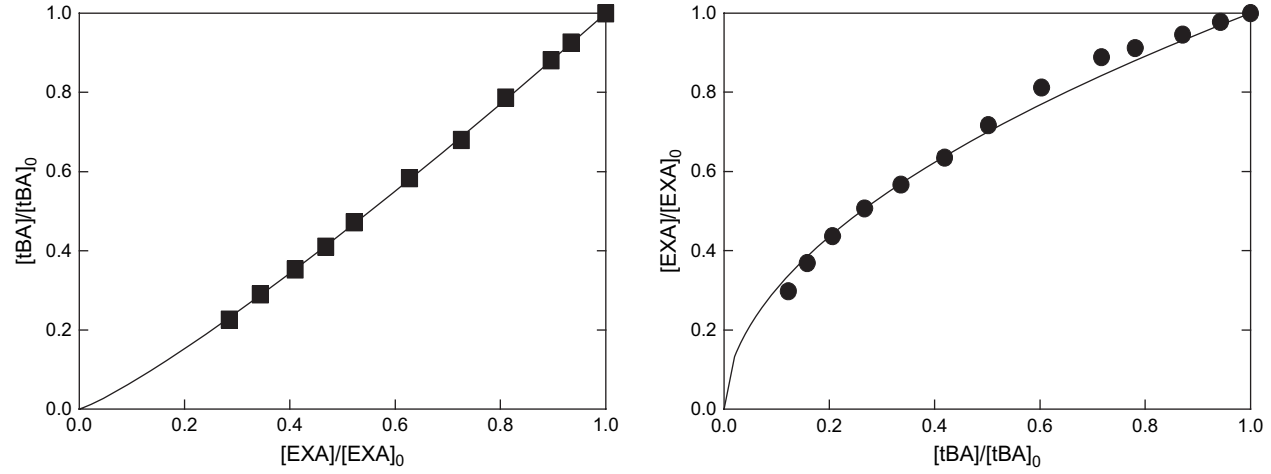

Fig. 2. Variation in concentration ratio $[M_1]/[M_1]_0$ of monomer 1 vs. that $[M_2]/[M_2]_0$ of monomer 2 during ATRCP in tol-d_8. In the *left* plot monomers 1 and 2 are tBA and EXA, respectively. In the *right* plot monomers 1 and 2 are EXA and tBA, respectively.

Table 2
Comparison of characteristics of a P(EXA-*r*-*t*BA)-Br sample and its fractions

Sample	SEC $M_n \times 10^{-4}$	SEC M_w/M_n	Mass (g)
Original	2.3	1.25	23.9
Fraction 1	2.7	1.19	2.0
Fraction 2	2.5	1.17	17.6
Fraction 3	1.5	1.25	3.8

seven P(EXA-*r*-*t*BA)-PCEA samples (Table 3). Fig. 4 shows a ^{1}H NMR spectrum and polymer peak assignments for sample 5 in Table 3. From the ratio of intensities of peaks at 3.96 and 4.30 ppm we obtained an *n*/*m* value of 1.42. The *tert*-butyl peak of *t*BA is not well resolved here for its low content and the *t*BA content *x* of 0.5 mol% shown in Table 3 is actually its feed molar ratio. Aside from ^{1}H NMR analysis, we also determined in THF the specific refractive index increment dn_r/dc, the LS weight-average molar mass M_w, and SEC polydispersity M_w/M_n for this sample and for the other samples. Combining the NMR *n*/*m* and the LS M_w values we calculated the weight-average numbers of repeat units n_w and m_w for the first and second blocks of each diblock with results given in Table 3. The fact that most of the samples possessed low polydispersity and sample 6 with a total of more than 700 monomer units still possessed a low polydispersity of 1.27 suggests prowess of ATRP.

3.4. Composition dependence of dn_r/dc

Different P(EXA-*r*-*t*BA)-PCEA diblocks were prepared to facilitate examination of how block copolymer composition changes affected the morphology and size of micelles formed from this series of diblocks in block-selective solvents such as EHC-45 oil and then the friction performance properties of the resultant particles. The availability of such diblocks also allowed us to examine how the specific refractive index increments dn_r/dc of the diblocks varied with the weight fraction of EXA or w_X in the diblocks (Fig. 5), where w_X was calculated by treating *t*BA as EXA and thus approximating P(EXA-*r*-*t*BA)-PCEA by PEXA-PCEA for the low *t*BA contents in the diblocks. To enable a more precise regression analysis we have determined also the dn_r/dc values for P(EXA-*r*-*t*BA)-Br (sample 3 in Table 1) and a PCEA sample with $m \approx 150$. The dn_r/dc values of a total of nine samples were fitted by the following relation:

$$\frac{dn_r}{dc} = 0.150 - 0.0845 w_X \,(\mathrm{mL/g}) \tag{5}$$

A linear relation between dn_r/dc and the weight fractions of one monomer in a series of diblocks is in agreement with prior observations made on other polymers [44]. The data of Fig. 5 do not all fall on the straight line probably due to experimental errors in the dn_r/dc values and also due to the use of samples with different but not necessarily high molar masses. It is well known that most polymer properties including their refractive indices are molar mass dependent. Asymptotic values are reached only for high molar mass samples. Nonetheless, Eq. (5) should be useful in the future for the calculation of dn_r/dc values of any P(EXA-*r*-*t*BA)-PCEA samples provided that *t*BA content is low and the molar masses of the samples are sufficiently high, e.g. >50,000 g/mol. This equation should

Table 3
Characteristics of some P(EXA-*r*-*t*BA)-PCEA samples prepared

Sample	dn_r/dc (mL/g)	LS $M_w \times 10^{-4}$ (g/mol)	SEC M_w/M_n	NMR *n*/*m*	n_w	m_w	*x* (%)
1	0.107	8.6	1.24	1.53	235	150	1.5
2	0.101	9.8	1.24	1.73	275	160	1.5
3	0.120	11.6	1.39	0.88	250	290	0.3
4	0.128	13.2	1.50	0.44	200	450	0.3
5	0.107	11.8	1.30	1.42	310	220	0.5
6	0.121	15.8	1.27	0.82	335	410	0.5
7	0.095	10.4	1.16	2.38	320	135	0.1

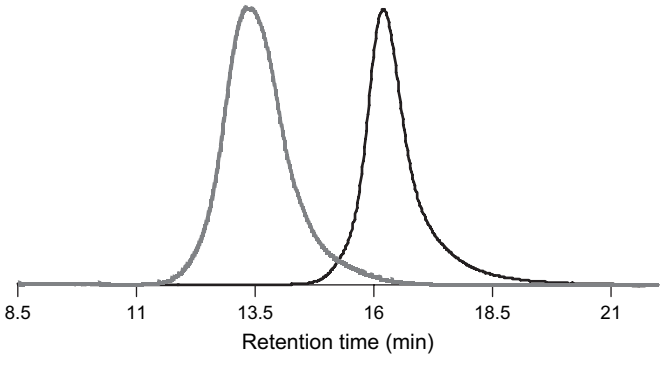

Fig. 3. Comparison of SEC traces for a P(EXA-*r*-*t*BA)-Br sample (dark curve) and its diblock P(EXA-*r*-*t*BA)-P(HEA-TMS) (gray curve).

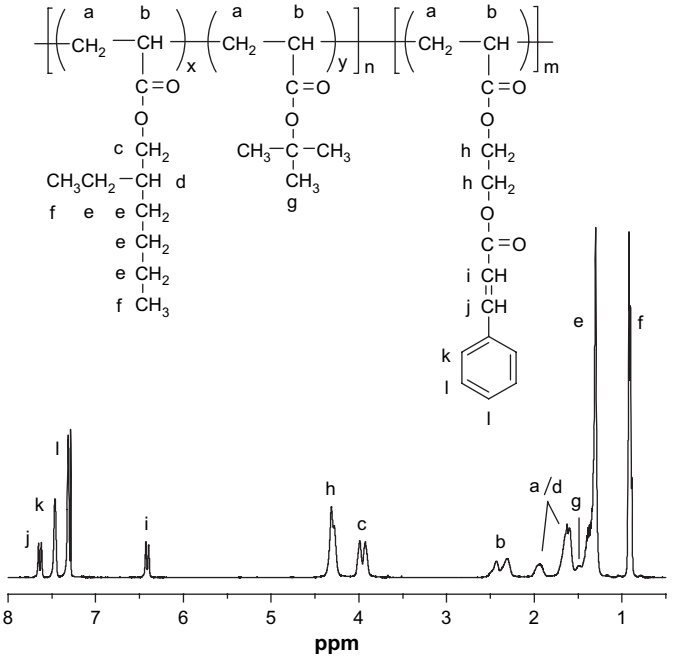

Fig. 4. Proton NMR spectrum of P(EXA-*r*-*t*BA)-PCEA (sample 5 in Table 3) in $CDCl_3$.

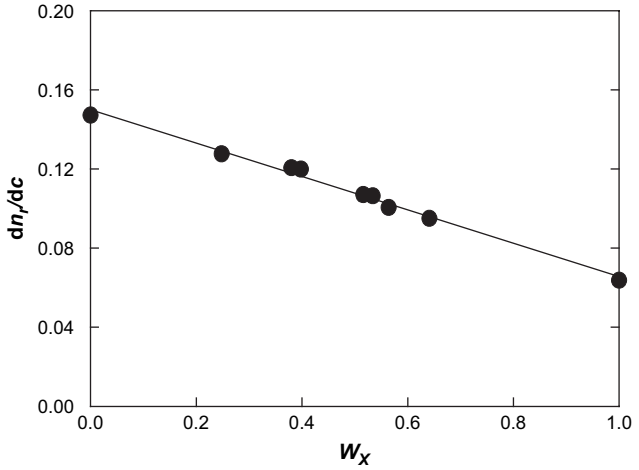

Fig. 5. Variation in dn_r/dc of P(EXA-*r*-*t*BA)-PCEA samples as a function of w_X in THF.

be useful, in principle, also for determining polymer composition from dn_r/dc analysis.

3.5. Thermal properties

Fig. 6 compares the TGA curves of P(EXA-*r*-*t*BA)-Br (sample 3 in Table 1), PCEA with $m \approx 150$, and P(EXA-*r*-*t*BA)-PCEA (samples 1 and 6 in Table 3). Interestingly, PCEA is thermally more stable than P(EXA-*r*-*t*BA)-Br and the diblocks are more stable than the P(EXA-*r*-*t*BA)-Br and PCEA polymers.

Fig. 7 shows DSC traces for PCEA with $m \approx 150$ and P(EXA-*r*-*t*BA)-PCEA (samples 1 and 6 in Table 3). The glass transition temperatures T_g seen between 26 and 30 °C must belong to PCEA. The fact that the PCEA T_g changed little from homopolymer to block copolymers suggests phase segregation between PCEA and P(EXA-*r*-*t*BA) in the solid state. We have also analysed P(EXA-*r*-*t*BA)-Br (sample 3 in Table 1) and found no glass transition for this sample in the temperature range between −60 and 150 °C. This suggests that its T_g must be lower than −60 °C in agreement with $T_g = -65$ °C reported by Gonzalez-Leon et al. [45].

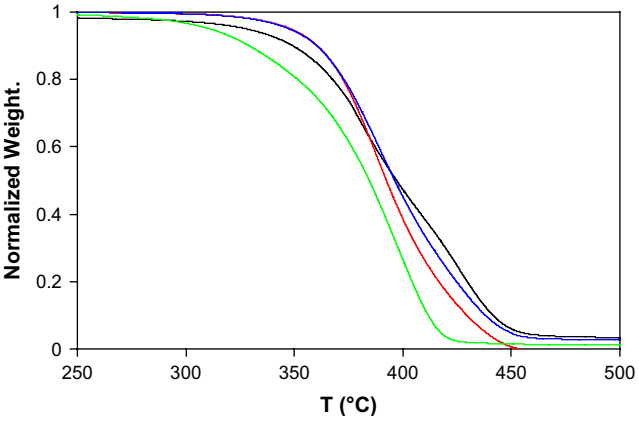

Fig. 6. Comparison of TGA curves of P(EXA-*r*-*t*BA)-Br (sample 3 in Table 1) (green), PCEA with m ≈ 150 (black), P(EXA-*r*-*t*BA)-PCEA (samples 1 (red) and 6 (blue) in Table 3).

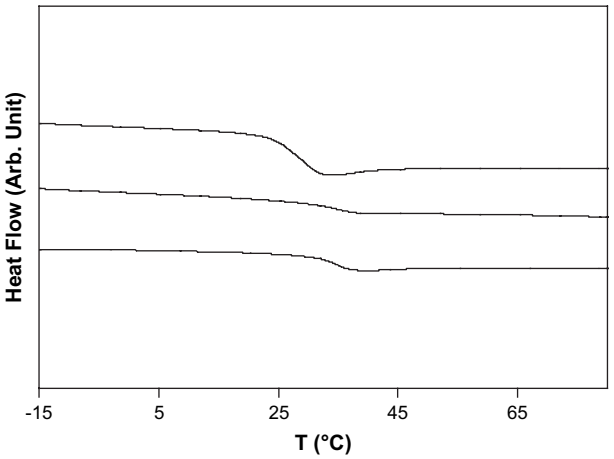

Fig. 7. DSC traces for PCEA with $m = 150$ (top), P(EXA-*r*-*t*BA)-PCEA (samples 1 (middle) and 6 (bottom) in Table 3).

3.6. Micelle formation

Visual inspection of the structures of PEXA and PCEA revealed that PEXA should be less polar than PCEA and less polar solvents like CH and EHC-45 oil should be block-selective for PEXA. This intuition was supported by the solubility parameters δ of 20.2 and 17.8 $J^{1/2}/cm^{3/2}$ for PCEA and PEXA that we calculated based on group contributions to molar cohesive energy and volume of the polymers [46] and verified by direct solubility test.

For the block-selectiveness of CH and EHC-45 oil we were able to prepare micelles or nanoaggregates from P(EXA-*r*-*t*BA)-PCEA by stirring them directly in CH with $\delta = 16.8$ $J^{1/2}/cm^{3/2}$ [44] and EHC-45 oil at high temperatures. Fig. 8 shows TEM images of micelles of P(EXA-*r*-*t*BA)-PCEA (sample 7 in Table 3) prepared in and sprayed from EHC-45 oil and CH, respectively. The spherical nanoaggregates prepared in CH are very uniform in size with an average diameter of 37 ± 4 nm. This size uniformity is typical of diblock micelles that have been studied by many groups before. A mixture of spheres with diameter of 37 ± 3 nm and cylinders with diameter of 28 ± 4 nm is seen for the sample prepared in EHC-45 oil. This difference in nanoaggregate morphology in EHC-45 oil may have two reasons. First, the cylindrical aggregates may be kinetic product for the high viscosity of the oil. Second, the cylindrical aggregates might be thermodynamically favored micelles. If they are micelles, this suggests that EHC-45 is a worse solvent for PCEA than CH [47].

Photocrosslinking of PCEMA and PCEA has been used by us in the past to prepare various ‘‘permanent’’ or crosslinked nanostructures as well as ‘‘sculptured permanent’’ nanostructures with certain domain(s) degraded and other(s) crosslinked including nanospheres [43], hollow nanospheres [48,49], nanofibers [50,51], nanotubes [12,52], supersurfactant [53], nanotube multiblocks [54], and thin films containing nanochannels

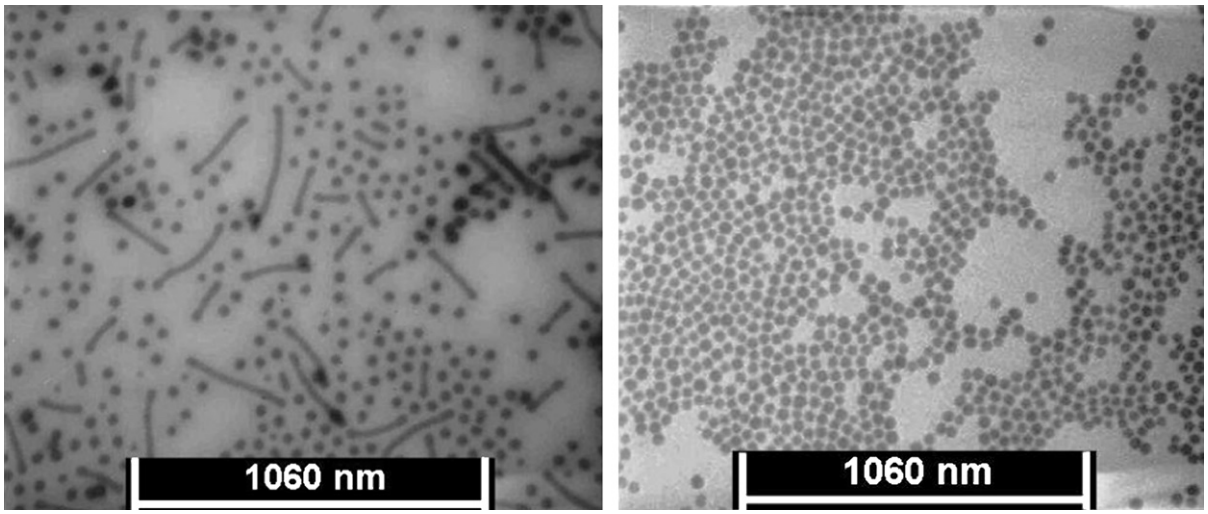

Fig. 8. TEM images of micelles prepared in and aspirated from EHC-45 oil (left) and cyclohexane (right), respectively.

[55,56]. The equal effectiveness of PCEA crosslinking here was demonstrated by the insolubility of these particles in THF after their irradiation by UV light [43].

4. Conclusions

P(EXA-*r*-*t*BA)-Br with low polydispersity has been successfully synthesized by ATRCP. Kinetics of the copolymerization performed in tol-d_8 were followed by ^{1}H NMR. Analysis of the kinetic data yielded the reactivity ratios r_{EXA} and r_{tBA} of 0.52 and 1.16, respectively. The macro-initiator P(EXA-*r*-*t*BA)-Br synthesized from ATRCP functioned well in initiating the controlled ATRP of HEA-TMS. The resultant P(EXA-*r*-*t*BA)-P(HEA-TMS) polymers were readily converted to P(EXA-*r*-*t*BA)-PCEA via first P(HEA-TMS) hydrolysis and then cinnamation of the PHEA block. Our detailed characterization of a series of P(EXA-*r*-*t*BA)-PCEA samples allowed the establishment of an equation governing the dn_r/dc dependence of such diblocks on their compositions. We also showed that the P(EXA-*r*-*t*BA)-PCEA diblock was highly stable thermally and the glass transition temperature of PCEA was low between 26 and 30 °C. Finally, P(EXA-*r*-*t*BA)-PCEA could be used to prepare nanoaggregates or micelles by dispersing the polymers in hot EHC-45 oil directly.

Acknowledgements

Afton Chemical Corporation and the Collaborative Research and Development Program of the Natural Sciences and Engineering Research Council of Canada are gratefully acknowledged for financially sponsoring this research. Jiandong Wang is thanked for carrying out the light scattering analyses and John Dupont is thanked for taking the TEM images.

References

[1] Wang JS, Matyjaszewski K. J Am Chem Soc 1995;117:5614.
[2] Matyjaszewski K, Xia JH. Chem Rev 2001;101:2921.
[3] Cai YL, Armes SP. Macromolecules 2004;37:7116.
[4] Zhang WQ, Shi LQ, An YL, Gao LC, Wu K, Ma RJ, et al. Macromol Chem Phys 2004;205:2017.
[5] Lazzari M, Liu GJ, Lecommandoux S. Block copolymers in nanoscience. Weinheim, Germany: Wiley-VCH; 2006.
[6] Tuzar Z, Kratochvil P. Surf Colloid Sci 1993;15:1.
[7] Forster S, Antonietti M. Adv Mater 1998;10:195.
[8] Canham PA, Lally TP, Price C, Stubbersfield RB. J Chem Soc Faraday Trans 1980;76:1857.
[9] Zhang LF, Eisenberg A. Science 1995;268:1728.
[10] Ding JF, Liu GJ, Yang ML. Polymer 1997;38:5497.
[11] Yu K, Eisenberg A. Macromolecules 1998;31:3509.
[12] Stewart S, Liu G. Angew Chem Int Ed Engl 2000;39:340.
[13] Raez J, Barjovanu R, Massey JA, Winnik MA, Manners I. Angew Chem Int Ed Engl 2000;39:3862.
[14] Frankowski DJ, Raez J, Manners I, Winnik MA, Khan SA, Spontak RJ. Langmuir 2004;20:9304.
[15] Grumelard J, Taubert A, Meier W. Chem Commun 2004:1462.
[16] Jenekhe SA, Chen XL. Science 1999;283:372.
[17] Ding JF, Liu GJ. Macromolecules 1997;30:655.
[18] Opsteen JA, Cornelissen J, van Hest JCM. Pure Appl Chem 2004; 76:1309.
[19] Checot F, Lecommandoux S, Gnanou Y, Klok HA. Angew Chem Int Ed Engl 2002;41:1339.
[20] Pochan DJ, Chen ZY, Cui HG, Hales K, Qi K, Wooley KL. Science 2004;306:94.
[21] Zhu JT, Liao YG, Jiang W. Langmuir 2004;20:3809.
[22] Cameron NS, Corbierre MK, Eisenberg A. Can J Chem 1999;77:1311.
[23] Price C, Hudd AL, Stubbersfield RB, Wright B. Polymer 1980;21:9.
[24] Wills JG. Lubrication fundamentals. New York: Mercel Dekker, Inc.; 1980.
[25] Zheng RHL, Wang Jiandong, Liu Guojun, Jao TC. Macromolecules 2007;40:7601.
[26] Muhlebach A, Gaynor SG, Matyjaszewski K. Macromolecules 1998;31:6046.
[27] Matyjaszewski K, Patten TE, Xia JH. J Am Chem Soc 1997;119:674.
[28] Erickson D, Lu FZ, Li DQ, White T, Gao J. Exp Therm Fluid Sci 2002;25:623.
[29] Davis KA, Matyjaszewski K. Macromolecules 2000;33:4039.
[30] Ma QG, Wooley KL. J Polym Sci Part A Polym Chem 2000;38:4805.
[31] Bednarek M, Biedron T, Kubisa P. Macromol Rapid Commun 1999;20:59.
[32] Lu ZH, Liu GJ, Duncan S. Macromolecules 2004;37:174.
[33] Liu GJ, Yan XH, Lu ZH, Curda SA, Lal J. Chem Mater 2005;17:4985.

[34] Jo SM, Gaynor SG, Matyjaszewski K. Abstr Pap Am Chem Soc 1996;212:91.
[35] Bicak N, Ozlem M. J Polym Sci Part A Polym Chem 2003;41:3457.
[36] Vidts KRM, Dervaux B, Du Prez FE. Polymer 2006;47:6028.
[37] Lad J, Harrisson S, Mantovani G, Haddleton DM. Dalton Trans 2003:4175.
[38] Gromada J, Spanswick J, Matyjaszewski K. Macromol Chem Phys 2004;205:551.
[39] Qiu XP, Liu GJ. Polymer 2004;45:7203.
[40] Liu G, Yang H, Zhou J, Law SJ, Jiang Q, Yang G. Biomacromolecules 2005;6:1280.
[41] Coca S, Jasieczek CB, Beers KL, Matyjaszewski K. J Polym Sci Part A Polym Chem 1998;36:1417.
[42] Cai YL, Tang YQ, Armes SP. Macromolecules 2004;37:9728.
[43] Guo A, Liu GJ, Tao J. Macromolecules 1996;29:2487.
[44] Brandrup J, Immergut EH. Polymer handbook. 3rd ed. New York: John Wiley & Sons; 1989.
[45] Gonzalez-Leon JA, Ryu SW, Hewlett SA, Ibrahim SH, Mayes AM. Macromolecules 2005;38:8036.
[46] van Krevelen DW. Properties of polymers – their correlation with chemical structure; their numerical estimation and prediction from additive group contributions. 3rd ed. Amsterdam: Elsevier Science; 1997.
[47] Bang J, Jain SM, Li ZB, Lodge TP, Pedersen JS, Kesselman E, et al. Macromolecules 2006;39:1199.
[48] Ding JF, Liu GJ. J Phys Chem B 1998;102:6107.
[49] Stewart S, Liu GJ. Chem Mater 1999;11:1048.
[50] Liu GJ, Qiao LJ, Guo A. Macromolecules 1996;29:5508.
[51] Liu GJ, Ding JF, Qiao LJ, Guo A, Dymov BP, Gleeson JT, et al. Chem Eur J 1999;5:2740.
[52] Yan XH, Liu GJ, Liu FT, Tang BZ, Peng H, Pakhomov AB, et al. Angew Chem Int Ed Engl 2001;40:3593.
[53] Liu G, Yan X, Li Z, Zhou J, Duncan S. J Am Chem Soc 2003;125:14039.
[54] Yan XH, Liu GJ, Li Z. J Am Chem Soc 2004;126:10059.
[55] Liu GJ, Ding JF, Guo A, Herfort M, BazettJones D. Macromolecules 1997;30:1851.
[56] Liu GJ, Ding JF, Hashimoto T, Kimishima K, Winnik FM, Nigam S. Chem Mater 1999;11:2233.